Development and calibration of a low cost radar testbed based on the Universal Software Radio Peripheral

Jonas Myhre Christiansen Norwegian Defence Research Establishment
Kjeller, Norway
Email: Jonas-Myhre.Christiansen@ffi.no
Graeme E. Smith The Ohio State University
Columbus, Ohio, USA
Email: smith.8347@osu.edu

***Abstract*—For a cognitive radar algorithm to be useful, it must run on radar hardware that is flexible. Typically, this has been viewed as requiring a software defined radio (SDR). With the emergence of cheap, digital transceiver systems, such as the Universal Software Radio Peripheral (USRP) from Ettus, these systems are cheaper than ever to produce. This article reports on the development of a USRP based radar system. Calibration testing for radar cross section (RCS) is undertaken. The phase noise is characterized as having a standard deviation of 0.02 radians. Detections of commercial aircraft at ranges up to 5.5 km are demonstrated. An adaptive update interval tracking experiment, using the fully adaptive radar (FAR) framework for cognitive radar, is reported on. In this experiment a small unmanned aerial vehicle (UAV) is detected at ranges of up to 300 m. Using the radar equation with a signal loss proportional to R^{-4}, the interpolated maximum detection range is approximately 600 m.**

I. Introduction

This article presents the development, calibration, and preliminary testing of a software defined radio (SDR) suitable for use as a cognitive radar testbed. Experimental testbeds are critical for cognitive radar research. The dynamic response of the radar to the environment limits the suitability of simulations and prerecorded data for testing. If a simulation is used, it would require a very high degree of fidelity. Realistic models of clutter and target are needed at a level suitable to simulate received waveforms on a pulse-by-pulse basis. Such low level modeling is possible, but results in high processing overheads and long run times. When prerecorded data is used, it must be oversampled such that the cognitive radar processing can demonstrate adaption by subsampling. Such methods can work, as shown by Bell [1] and Mitchell [2], but place limitations on what can be achieved. Further, there are few publically available datasets with suitable oversampling. A previous article by Smith [3], introduced the cognitive radar engineering workspace (CREW) system developed by The Ohio State University. While the CREW system has been invaluable for conducting cognitive radar research [4], [5], it is cost prohibitive for widespread deployment. Here, we report on a smaller form-factor testbed that uses a Universal Software Radio Peripheral (USRP) [6] for its digital backend, and can be fabricated for a few thousand dollars.

Research on USRP's and other SDR platforms has been reported for several years, with a notable uptick in such publications since 2011. An article from 2011 [7] demonstrated a USRP based frequency modulated continuous wave (FMCW) radar for weather surveillance applications. It demonstrated the ability to detect multiple targets using delay lines in a loop-back configuration. Moreno et al. [8] discussed the potential for USRP based radar, and demonstrated an experimental characterization of a system based on a USRP NI2920. Other work [9] demonstrated a simple experimental radar using the USRP B210. It showed range profiles with target responses attributed to a large building. These publications show the potential of using USRP's in experimental testbeds for radar. Kirk et al. [10] have used the USRP in an experimental radar system for a cognitive radar (CR) application focusing on radio frequency interference (RFI) mitigation. The method introduces notches into the transmit waveform bandwidth based on the sensed spectral environment. This requires notching the spectral content of the waveform on a pulse-by-pulse basis, and hence the timing requirement is extreme. Previous work by the authors [11] demonstrated an experimental radar system with detection performance for air targets of several kilometers. There, adaptive pulse repetition frequency (PRF) selection on a dwell-by-dwell basis was demonstrated and the flexibility of selecting waveform parameters was explained.

SDRs are attractive because they increase the flexibility of radar systems. When the radar's architecture is defined in software, it is easy to change. Developing radars that have different operating modes becomes much easier than hard coded systems, where waveforms and other parameters requires more effort to change. Alternatively, the same physical system can be deployed for a completely different activity by downloading new software to it. Invariably, there is some radio frequency (RF) hardware that remains. The more flexible this is made, the more diverse the operating modes and uses of the radar can be. The flexible RF front-end can be viewed as providing a large parameter space for the radar to operate in. The precise parameter selections are

Dette er en postprint-versjon/This is a postprint version.
DOI til publisert versjon/DOI to published version: 10.1109/MAES.2019.2953803

then a function of the software. It is the presence of this large, selectable parameter space that gives rise to a desire to make radars cognitive. In an ideal situation, the radar parameter selections would be matched to the environment to maximize performance—for example, avoid interference, maximize SINR, minimize track variance etc. The designer cannot know ahead of time what the environment will be to a sufficient level of detail to match the parameter selections to it. Instead, if performance is to be maximized, the radar must decide autonomously how to utilize the parameter space in response to the environment measurements it is making. It is this need to autonomously decide on operating parameters that leads to the field of cognitive radar.

The best example available for system performance optimization in response to stimuli is human cognition [12]. In human cognition, sensory inputs are processed through the central nervous system and result in actions being undertaken. When the actions are executed the relation of the person to the environment changes, and the sensory inputs change accordingly. New actions are then decided on and executed. This process continues in an endless cycle. Parallels can be drawn to radar sensing using SDR with a large parameter space and an algorithm that decides radar parameters based on perceptions. The rise of the SDR and the interest in cognitive radar therefore go hand in hand.

This article shows the development and characterization of a radar testbed based on the USRP, that allows testing of some adaptive or cognitive algorithms. The testbed is flexible in parameter selection, that allows for selection of radar parameters on a dwell-by-dwell basis. As shown previously in this section, such a testbed is important in the field of cognitive and adaptive radar since the selection algorithms usually are dependent on the environment in some sense. The testbed is relatively low cost.

To put SDR used in radar in context with the field of adaptive and CR, Section I introduced SDR, adaptive and cognitive radar research. Section II shows the hardware of the testbed, and explains how it is put together. Section III introduces the software architecture, the language and libraries used in the radar program. It also contains a link to the entire radar software available from Github. Section IV shows a radar cross section (RCS) calibration of the system, together with a system characterization. Section V shows some results from a set of experiments performed using the radar testbed. Both detection ranges for different targets, and the use of adaptivity on track update interval is introduced. Section VI discusses the conclusions of the development of the testbed.

II. Hardware

The SDR system reported on in this article uses the USRP X310 from Ettus as its digital back end. The X310 was selected due to its high sampling rate, two input channels, and the quality of RF front-end cards. The principles of the development shown in this article apply to all USRPs using the USRP Hardware Driver (UHD) library, but with some limitations on sampling rate, number of channels or RF front-end cards.

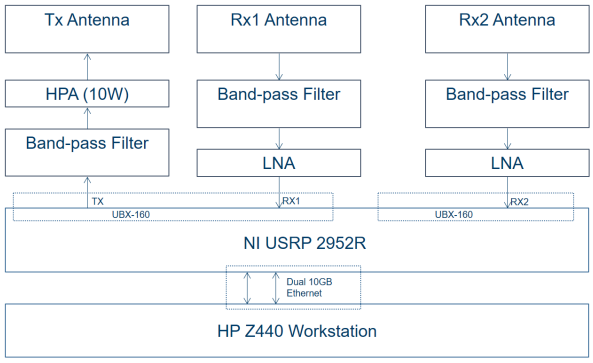

Figure 1: Block diagram of the cognitive radar SDR system

Figure 1 shows a block diagram of the system, and images of the different components are given in Figure 2. A list of components is given in table I.

A. Software Defined Radio

The USRP X310 is a device with an Field-Programmable Gate Array (FPGA) and two analog-to-digital converters (ADCs) and two Digital-to-Analog Converters (DACs) devices. It supports sampling rates up to 200 MS/s with IQ modulation, and hence it can sample a bandwidth of up to 200 MHz at 14 bit in receive and 16 bit at transmit. RF front-end cards can be inserted, which enables the device to sample at RF frequencies supported by the different cards. Software controlled amplification and local oscillator (LO) is available to fine tune the signal on both transmit and receive. The device used in this testbed has the UBX-160 cards inserted, which allows it to cover a 160 MHz bandwidth tune-able between 400 MHz and 6 GHz. The carrier frequency is software controlled, as most of the tunable parameters are. This allows for a highly flexible device for transmitting and receiving signals, and hence it should be well suited for radar applications.

The device is controlled by a host computer through a

Type	Manufacturer	Model
Workstation	HP	Z440
2x 10Gb PCI-express card	Intel	783345-01
2x 10Gb SFP Ethernet cables	Generic	Na
USRP	Ettus	X310
2x USRP RF Frontend cards	Ettus	UBX-160 card
High power amplifier	MiniCircuits	ZVE-8G+
2x LNA	MiniCircuits	PSA4-5043+ on TB-653+
3x S-band bandpass filters	K&L	8FV40-3200/T200-O/O
2x S-band E-patch RX antennas	Generic	Na
1x S-band E-patch TX antenna	Generic	Na
SMA cables	Generic	Na
12V DC Supply	Generic	Na
12V-5V DC-DC converter	Generic	Na
Weather proof box	Generic	Na

Table I: SDR parts list

Dette er en postprint-versjon/This is a postprint version.
DOI til publisert versjon/DOI to published version: 10.1109/MAES.2019.2953803

dual 10 Gbps Ethernet connection, which allows for a high data transfer rate between host and the device. The connection itself supports transmit and receive at full bandwidth on two channels. The limiting factor is the host computer which has to process all the data. The host computer controls the device through the UHD library, which supports functions communicating with the FPGA on-board the device. All functions called on the FPGA are pre-defined from Ettus and are contained in the FPGA binary image supplied by Ettus. There is no need for FPGA programming, and hence the development can be performed in languages supported by the UHD library which is easier to develop and debug than developing FPGA functions.

B. RF equipment

To achieve long detection ranges in a pulsed mode, a power amplifier is used. The MiniCircuits ZVE-8G+ [13] amplifier with an third order intermodulation product (IP-3) [14] of approximately 10 Watts is used producing a 20 dB amplification over the maximum output power of the SDR, given in Table II. The amplifier can be run in a saturated mode when operating at a maximum output power and to avoid non-linearities a cosine based waveform must be used. Single tone pulses, linear chirps and non-linear chirps are acceptable waveforms. If the amplifier is operated below the compression point, non-constant modulus waveforms such as orthogonal frequency division multiplexing (OFDM) [15] and noise pulses can be used.

The antenna subsystem consists of an E-patch antenna array with two elements spaced by approximately half a wavelength for angle-of-arrival (AOA) measurements. The manufactured transmitter antenna is an E-patch antenna mounted with a short distance from the receiver array to provide isolation between transmitter and receiver channels.

To calculate the angle from bore-sight for detected targets, we can use an AOA calculation exploiting the measured phase difference for the receiver antennas. If we define the element spacing to be L, the angle from bore sight to be θ, the phase difference measured between the antennas to be ϕ and the wavelength to be λ, the angle can be calculated as follows:

$$\phi = 2\pi\frac{L}{\lambda}\sin(\theta) \Rightarrow \theta = \sin^{-1}\left(\frac{\phi}{2\pi}\frac{\lambda}{L}\right) \tag{1}$$

From this, the unambiguous angle can be calculated setting $\phi = \pm\pi$:

$$\theta_{max} = \sin^{-1}\left(\frac{\pi}{2\pi}\frac{\lambda}{L}\right) = \sin^{-1}\left(\frac{\lambda}{2L}\right) \tag{2}$$

The receiver antennas are mounted with a spacing of 5.5cm, which is 0.58 times the wavelength at 3.15GHz. The calculated unambiguous angle is $\pm 59.7°$. The simulated antenna diagram showed a 10dB loss at $\approx \pm 60°$, and hence large targets may fold in through antenna side lobes.

The RF equipment is mounted in a weather proof box, shown in figure 2 (b) and connected to the SDR with coaxial cables. The antennas and box are mounted on a simple antenna rig depicted in figure 2 (a).

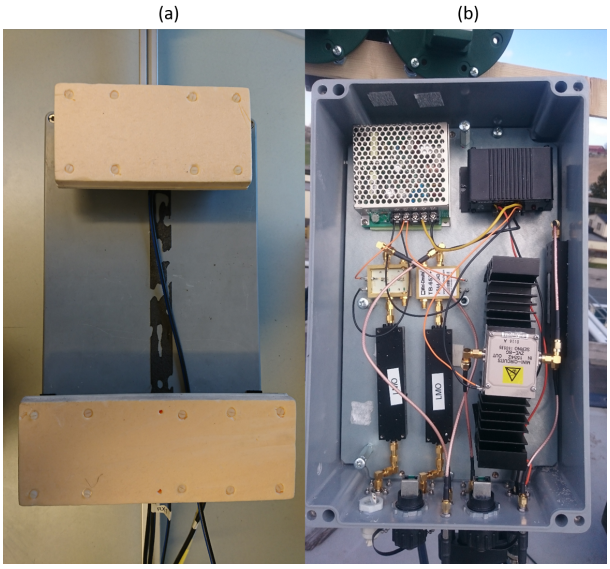

Figure 2: Pictures of the different components of the cognitive radar system; where (a) shows the antenna setup with the transmit antenna on top and receive antennas at the bottom, and (b) shows the RF front-end electronics with filters and amplifiers

C. Processing computer hardware

The radar's data processing system consists of three modules: a FPGA, a workstation, and a Graphical Processing Unit (GPU). The FPGA was part of the USRP and provides low level signal processing and control of the USRP hardware. Its most significant signal processing role is to perform Digital Down Conversion (DDC) of the received waveform so that true baseband can be passed to the workstation for further processing. Future implementation of the matched filter on the FPGA could be beneficial to free up resources on the GPU for its other tasks.

A GTX 1080 Ti GPU is used for processing that can be efficiently parallelized. Currently, this is the implementation of the matched filter, the discrete Fourier transform (DFT) required for Doppler and the Constant False Alarm Rate (CFAR) processing. Stages, such as detection clustering could be implemented in a parallel fashion on GPU. For the

USRP parameters	
Number of channels	2
Frequency range	400 MHz - 6 GHz
Maximum output power	100mW
Digital-to-Analog Converter (DAC) resolution	16 bit
analog-to-digital converter (ADC) resolution	14 bit
Noise figure	4-5 dB @ 3.1 GHz
Maximum instantaneous bandwidth	160 MHz TX and RX
Maximum I/Q sample rate	200 MS/s
Memory size	1024 MB

Table II: Ettus X310 with UBX-160 cards

Dette er en postprint-versjon/This is a postprint version.
DOI til publisert versjon/DOI to published version: 10.1109/MAES.2019.2953803

time being. However, they are implemented on the Central Processing Unit (CPU), where the CPU is a multi-core Intel Xeon processor of model E5-1650 with 6 cores running at 3.6 GHz.

III. Software

The USRP has several possibilities for software development. The most common approaches are:

- GNU Radio
- Matlab USRP support through Communication Toolbox
- LabView NI USRP module
- C++ UHD library
- Python wrapper for C++ UHD library

GNU Radio is a graphical radio programming interface that allows development with Python and C++. The initial investigation into using GNU Radio for radar applications showed that it was hard to get access to important features in the USRP. For example, the functionality required for phase synchronization between channels and synchronizing the signal between transmit and receive was not available.

Matlab has USRP support through the Communication Toolbox, although it contains a subset of the features available in the UHD library. These limitations lead to the conclusion that it was not the optimal development environment for a USRP based radar.

National Instruments (NI) LabView supports control of the USRP through the USRP module. In addition, LabView can be used to write software to run on the USRP's FPGA. The possibility of writing both controller and FPGA code in the same environment is a positive feature. Unfortunately, the engineering flexibility required for cognitive radar applications seems difficult to achieve in the LabView environment.

The C++ UHD library allows the necessary control of the USRP to create a radar system with pulse-to-pulse coherency and coherency between multiple channels. Pulse-to-pulse coherency is essential for Doppler processing, and coherency between channels are essential for AOA processing. Arbitrary signal generation in C++ is a straightforward task, and signal processing in C++/CUDA is also possible. The UHD library does not allow for programming the FPGA directly. However, implementation of blocks on the FPGA through the Xilinx Vivado is possible as is the use of the RF-network-on-a-chip (RFNoC) to place functionality on the FPGA. There are methods in the UHD library to allow access to these newly developed FPGA blocks. The outcome of the above evaluation was to select the C++ UHD environment to develop the USRP software defined radio (SDR). All programming comments in the remainder of this article should be taken as applying to this software development approach.

A Python wrapper of the C++ UHD library has been written, and it is shown to be slightly slower than a C++ implementation [16]. It does not currently support Ettus RFNoC, but it could be an interesting programming environment to consider for future development, since it allows the same control of the USRP as the C++ UHD library with the simplicity of programming in Python.

A. Software development environment dependencies

As shown in the previous section, the C++ UHD library was selected as the programming environment for developing the USRP radar. The UHD library allows for control of the USRP functions, such as setting up the radio, transmitting a time series, receiving data coherently over several channels and timing of the functions. The extra functionality needed in a radar system is the waveform generation which is done in C++ using the standard C++ library complex functions. Signal processing of the received data is done on the GPU using the CUDA programming language for parallel signal processing. The matrix operations needed in the Kalman filter tracker is supplied in the Boost library. Boost has many other features used in the program such as thread handling, timing and file system control. Qt and Qwt were used for the Graphical User Interface (GUI) and data display such as plan position indicator (PPI) and range-Doppler displays. Table III shows the software dependencies.

Library	Description
UHD [17]	UHD library
Qt [18]	Qt is used for GUI programming
Qwt [19]	Plotting library for Qt
Boost [20]	Boost C++ libraries
CUDA [21]	GPU programming library

Table III: List of dependent software libraries

B. Waveform generation

Waveform generation is done in a C++ class object, based on the complex number manipulation from the standard library. The only dependencies is the standard library functions for vector and complex numbers. Three waveforms are currently implemented; rectangular, Linear Frequency Modulation (LFM) and Non-Linear Frequency Modulation (NLFM) pulses. The waveform generation has run-time adjustable parameters such as pulse length, bandwidth, PRF and number of pulses generated. The waveform is generated on a dwell-by-dwell basis.

C. Range-Doppler processing

The range-Doppler processing is based on a matched filter implemented with zero filling, fast Fourier transform (FFT) and inverse fast Fourier transform (IFFT) for fast convolution in the range domain, and a FFT in the slow time domain for Doppler processing. The processing is standard for a range-Doppler radar, but the parallel nature of the processing allowed it to be efficiently implemented on a GPU. The GPU implementation introduced a speedup factor of 50 compared to the implementation on the CPU, even when using all 6 cores of the CPU. The use of the GPU allows an inexpensive workstation machine to perform real-time processing for radar applications.

Dette er en postprint-versjon/This is a postprint version.
DOI til publisert versjon/DOI to published version: 10.1109/MAES.2019.2953803

D. Detection processing

The detection processing implemented is the cell averaging CFAR (CA-CFAR) [22] which compares the cell under test (CUT) to an average of the signal power in a window of neighboring cells. If the CUT is above a given threshold, it is counted as a detection. The threshold is calculated to give a specified false alarm rate. This method allows for a constant false alarm rate detection against a varying noise floor [23]. The cell averaging can be implemented as a filter. The filter is applied through convolution that makes use of the FFT functions that can be optimized to run on the GPU. As such, the CA-CFAR can be implemented on the GPU to reduce runtime.

It should be noted that the CA-CFAR is likely to create more than one detection per target. This is common for the method. A clustering routine is used to identify individual targets from the multiple detection the CA-CFAR produces. At the current time, the clustering algorithm runs on the the CPU.

E. Angle estimation processing

The angle estimation processing is based on the multiple signal classification (MUSIC) [24] algorithm. With two elements in the antenna array and an assumption of only one target in the range-Doppler resolution cell. This assumption is reasonable since the resolution cells are 0.75 m by 0.39 m/s when the bandwidth is 160 MHz and the dwell time is 12.3 ms at 3.15 GHz carrier frequency, and it seems unlikely that two targets could exist in such a small cell. The method can be simplified to solve the trigonometric equation given in (1). The method is dependent on the measured phase difference of a target in the two antennas, the distance between the elements and the wavelength.

F. Tracker

The tracker is a range-Doppler tracker, where the measurement and state space is the range and range-rate (which is proportional to Doppler velocity). A linear motion model assumption is made. While such a simple motion model does not necessarily give the best track performance, it is a simple implementation and has proven successful in the research conducted so far. Track initialization is currently implemented by the radar operator via a manual mouse click on the detection in the GUI. There is a plan to implement a multiple hypothesis tracker with converted range, bearing and range rate measurement [25], but this is outside the scope of the current article.

G. Run-time considerations for signal processing

The new generation of gaming GPU's contains several thousands of cores combined with large memory, and can be regarded as extremely powerful for calculations. The price range for gaming GPU's is much lower than NVIDIA's Tesla and Quadro cards. As demonstrated here, a gaming GPU provide single point precision calculations at rates fast enough to conduct real-time radar signal processing. Most, if not all stages of the signal processing can be implemented in parallel. Parallel processing efficiently implemented on GPU is much faster than if implemented at CPU, and can even compete with processing on FPGA. The fast compilation and easy debugging allows it to be great platform for both development of new algorithms, but also achieve real-time requirements on the signal processing.

H. Software availability

The software reported on in this article for controlling the USRP, performing the radar signal processing and creating the GUI can be downloaded from Github[1] at https://github.com/jonasmc83/USRP_Software_defined_radar.

IV. Radar calibration

Radar calibration is critical for evaluating the performance of a new system. This section reports on the two calibration tests made of the USRP based radar to evaluate system performance. The first was RCS calibration. The second, receive channel phase characterization which is required for moving target indication and angular measurement performance prediction.

A. RCS calibration

The RCS calibration was performed against a small metal sphere in an open field environment. The sphere was a 100mm diameter solid stainless steel ball bearing, shown in Figure 3 (a). A RCS calculation of a 100mm diameter sphere is shown in Figure 3 (b), where the RCS for the carrier frequency 3.15GHz used in this article is -20dBsm. The small size of the sphere compared to the wavelength results in the scattering is in the resonance region. Due to the uncontrolled nature of the test environment, it was not possible to perform background subtraction that is common in RCS measurements to separate the calibration sphere from the clutter. Instead, the robustness of the ball bearing was exploited. It was thrown by a volunteer giving it a Doppler shift that allowed its response to be separated from the ground clutter.

A set of eight range positions were selected, and the volunteer threw the sphere 1-3 times at each range position. This gives a set of signal power measurements for the sphere as a function of range. These measurements are depicted in Figure 4, where each dot is a measurement. The scene used made it difficult to perform measurements closer than 230m, and the low RCS of the sphere made it hard to detect the sphere past 300m. The signal power variation is approximately 2-3dB. We can say that this is an absolute calibration using the knowledge of the sphere RCS calculated as -20dBsm, but due to variation in the measurements it is accurate to within 2-3dB. The line shows a $\frac{1}{r^4}$ curve fitted for the dataset of thrown spheres, and using the knowledge of the RCS to be -20dBsm the curve can be used for estimating the RCS of other targets.

[1] https://github.com/jonasmc83/USRP_Software_defined_radar

Dette er en postprint-versjon/This is a postprint version.
DOI til publisert versjon/DOI to published version: 10.1109/MAES.2019.2953803

(a) 100mm diameter solid stainless steel ball bearing sphere

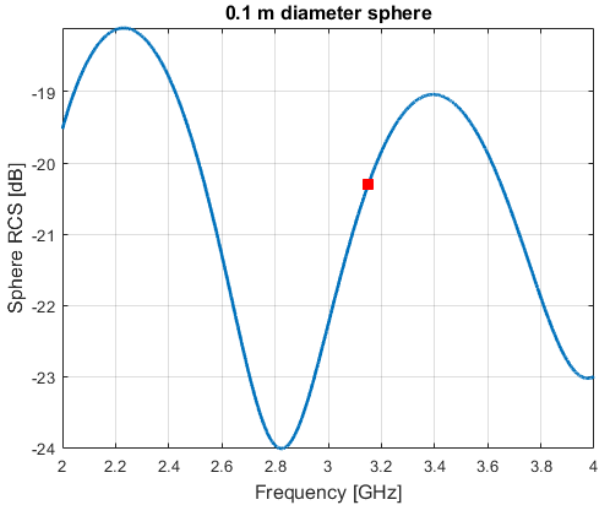

(b) RCS calculation of a 100mm diameter sphere; blue line is the calculated RCS in dBsm as a function of frequency, and the red square is the 3.15GHz point with value of -20.31dBsm

Figure 3

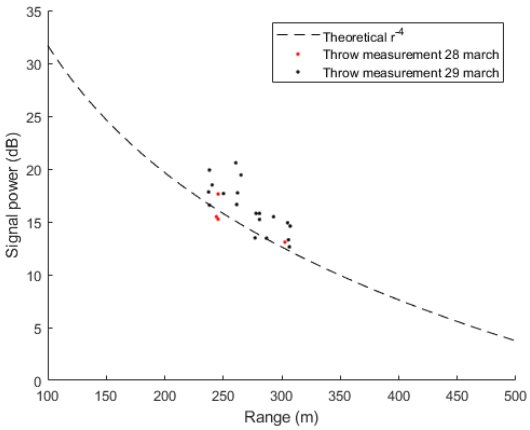

Figure 4: Measurements of thrown sphere at different ranges, shown as dots, compared to a $\frac{1}{r^4}$ curve from the radar equation. The $\frac{1}{r^4}$ curve is fitted to the measurements in an attempt to perform an absolute calibration of the radar system.

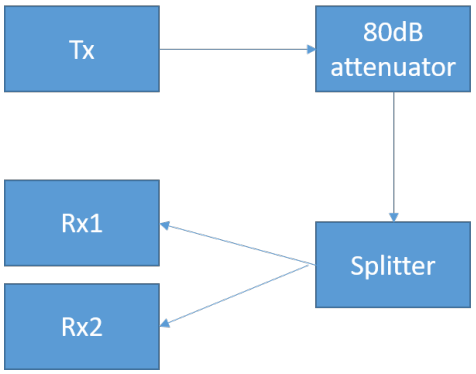

Figure 5: Diagram displaying the characterization setup, with a 80 dB attenuator and a power splitter to emulate a point target.

B. *Channel phase characterization*

The phase noise for each channel is a limiting factor in detection of slow moving targets close to the clutter ridge. The noise of the phase difference between channels is a limiting factor for angular estimation. A loop-back configuration to characterize the phase noise of each channel, and the phase difference between each channel, was set up. The loop-back configuration was achieved by disconnecting the antennas from the RF front-end, attaching two attenuators of 40 dB of total 80 dB attenuation and a power splitter to have two attenuated signal paths and then connecting the two signal paths to the receivers. This setup allows the transmit signal to be attenuated and fed into the two receiver stages, as shown in figure 5. The cable delay is less than one fast time sample, so this configuration produces an ideal target response at zero range. A measurement of the absolute phase noise of each channel were performed together with the phase difference between channels based on this response.

A dwell consists of a number of pulses, 4096 in this case. Each sample in figure 6 (a) shows 2 times the standard deviation calculated over these 4096 pulses, and hence the dashed curves shows an estimate of 2σ. The phase noise is similar for both channels, and this is expected since the channels are equal in the SDR and in the RF chain. Figure 6 (b) shows the same parameters as for (a), when looking at the phase difference of the two channels. The noise shown here directly affects the AOA measurement and will introduces uncertainty in the angular measurements. An error of 0.02 radians as given in figure 6 corresponds to approximately 0.3 degrees error in the angular estimate.

Dette er en postprint-versjon/This is a postprint version.
DOI til publisert versjon/DOI to published version: 10.1109/MAES.2019.2953803

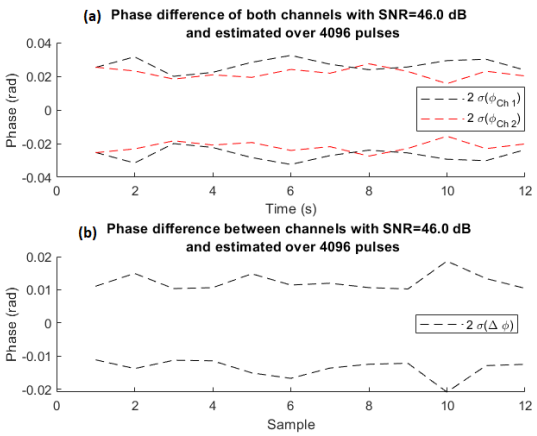

Figure 6: (a) shows the phase noise for each channel, and (b) shows the noise of the phase difference between channels.

The conclusion we can draw from this characterization is that the phase from pulse-to-pulse shows only a small variation due to phase noise. This implies coherency from pulse-to-pulse, and hence we can perform Doppler processing. The phase difference between channels is also constant, with a small variation due to phase noise. The implication from this is that we can do AOA for angular measurements, since the angular measurement is dependent on coherency between channels. The SDR radar system can therefore do Doppler and AOA processing.

V. Experimental results

A. Detection range

The system contains a 10W power amplifier and earlier predictions of the detection performance of this system [11] showed a substantial detection range, greater than 5 km for airliner size targets. The same prediction shows detection ranges of 3km and lower for smaller targets such as a light aircraft. Figure 7(a) shows a detection of a small aircraft at 2.8 km distance, and Figure 7(b) shows a detection of a large airliner aircraft detected at 5.5 km. This fits well with the previous predictions of the detection capabilities of this radar system.

B. Tracking small targets

The USRP radar is able to track small targets at short range. Using a short pulse allows it to monitor a surveillance volume close to the radar. An experiment with a small unmanned aerial vehicle (UAV)—a DJI Mavic—was performed. The pulse length was set to 0.8μs, which gives minimum range of 120 meters. The PRF was set to 100kHz, which gives an unambiguous range of 1.5km. The experiment is shown in Figure 8(a), which shows a picture of the UAV, a satellite photo of the test range and the position of the radar and track of the UAV. The UAV path in the overlay is the actual track of the UAV and it illustrates the angular accuracy of the AOA estimation. Figure 8(b) shows plots of the range, Doppler velocity and signal to noise ratio (SNR) of the UAV as it flies first outward, and then back towards the radar. The black dots are the radar detections and green squares are the tracker output. The tracker keeps track until 350m. It looses track when the target stops as it prepares to change direction. The lost track happens because the track merges into the stationary clutter and is not detected for several dwells. The operator starts a new track as soon as the target becomes separate from the clutter and the UAV is successfully tracked as it approaches the radar. Using the rule of thumb from the radar equation that a doubling in range corresponds to a 12dB drop in SNR, a detection range of 600m can be extrapolated.

C. Adaptive update interval method using the fully adaptive radar (FAR) framework

The paper by Christiansen [26] shows a method of calculating a track update based on a cost function to optimize some measure of resource usage, weighted against the global mean square error of the tracker [1]. The article shows the method applied on a simulated case. The method has been implemented on the USRP radar and the required interval until the next track update dynamically adapted based on the the predicted track error. The method was used in the case of the UAV track shown in the figures 8 (a) and (b). Figure 9(a) shows the tracker parameters of range uncertainty, velocity uncertainty and selected update interval respectively. The tracker uncertainty is relatively constant since the optimization method decreases the update interval as the target moves further from the radar. The measurement uncertainty increases when the target is further from the radar due to reduced SNR. The optimizer selects shorter update intervals since the tracker has lower state uncertainty with shorter update intervals and hence the global track error remains quite constant despite the SNR drop. Figure 9(b) shows the result of a cost function evaluation using the actual update interval selected for a 1 s fixed update interval experiment, and an experiment with adaptive update interval. The cost function values based on the true posterior information is smaller when using the adaptive update interval, a method which attempts to minimize this cost function based on predicted posterior information.

The experiment shown here is a work in progress. Research is already underway to expand the parameters adapted to include PRF and number of pulses in a dwell. The available parameters to optimize over in this SDR testbed are currently; carrier frequency, bandwidth, pulse length, PRF, number of pulses in dwell.

VI. Conclusion

The testbed shown in this article is based on the Universal Software Radio Peripheral (USRP) X-310, which is a member of a line of software defined radio (SDR)s available from Ettus. The USRPs are notable for their relatively low price and high levels of system configuration. The radio frequency (RF) hardware used for the front-end is all connectorized, commercial off the shelf. As such, it too is available at low cost and with minimal lead times.

Dette er en postprint-versjon/This is a postprint version.
DOI til publisert versjon/DOI to published version: 10.1109/MAES.2019.2953803

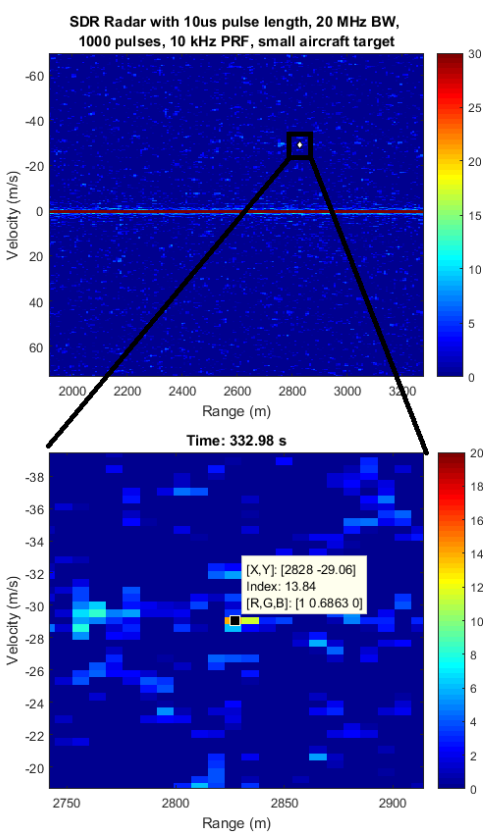

(a) Small aircraft detected at 2.8km distance with USRP based SDR radar system

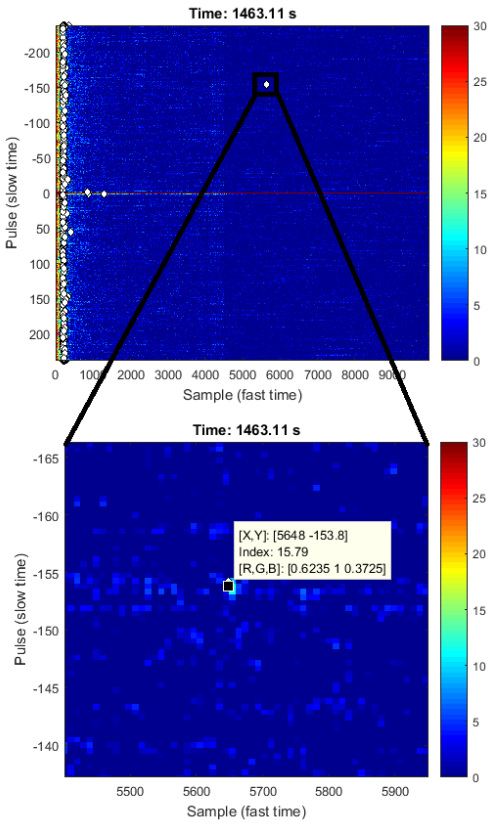

(b) Airliner type target (Boeing 737 class) detected at 5.5km distance with USRP based SDR radar system

Figure 7: Demonstration of detection ranges of the USRP based SDR radar system

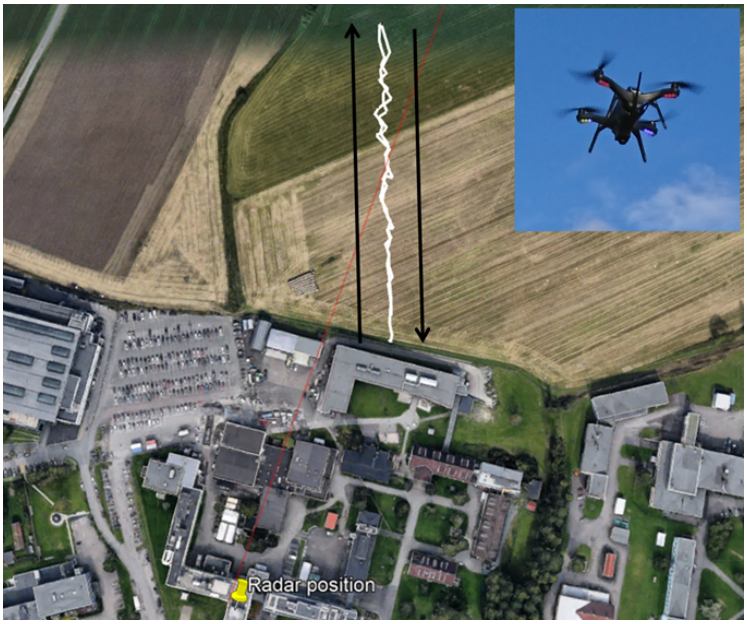

(a) Experimental setup of UAV flying outwards, turning, and flying inwards

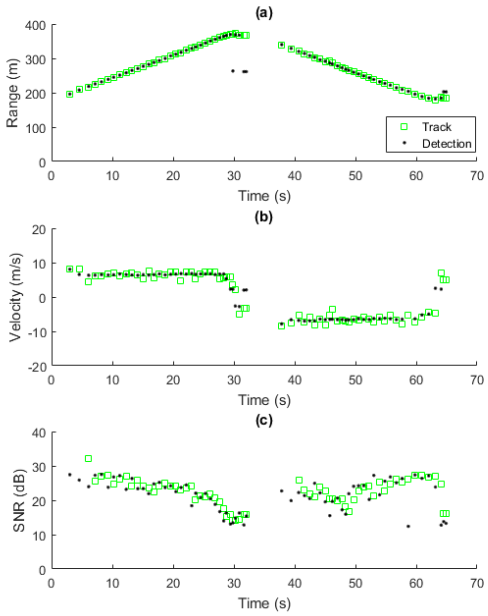

(b) Range, range-rate (Doppler velocity) and SNR plot respectively, from top to bottom

Figure 8: Experiment showing tracking of small UAV target out to 350m and back

Dette er en postprint-versjon/This is a postprint version.
DOI til publisert versjon/DOI to published version: 10.1109/MAES.2019.2953803

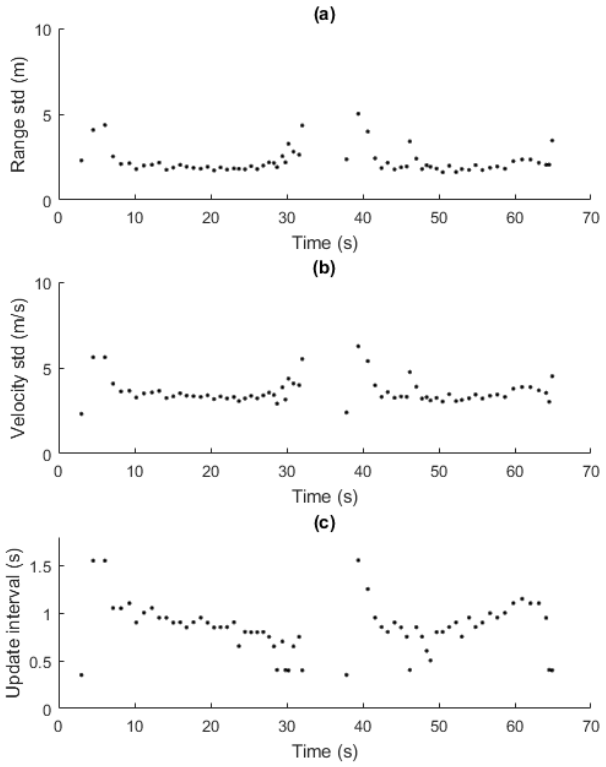

(a) Tracker parameters, with plots of range uncertainty, velocity uncertainty and the selected next update interval, respectively

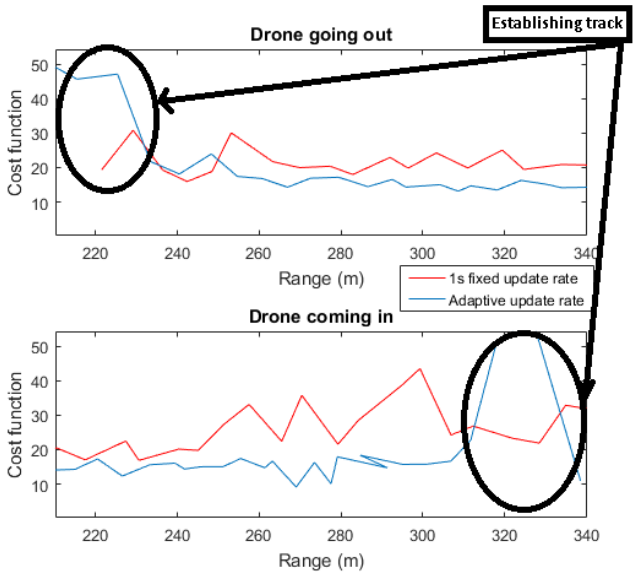

(b) Cost function values based on true posterior information for two experiments, where one experiment with fixed update interval of 1s is shown in red, and adaptive update interval is shown in blue.

Figure 9: Experiment showing tracking of small UAV target, with showing track parameters and cost function values

The testbed can therefore be kept at low cost and hence affordable to academia and smaller research projects. The software is based on the USRP Hardware Driver (UHD) driver library in C++ and CUDA code for signal processing. The program can therefore run on a workstation with a NVIDIA Graphical Processing Unit (GPU) installed. The source code for the entire radar project can be found at https://github.com/jonasmc83/USRP_Software_defined_radar.

The system calibration section introduced a method for absolute radar cross section (RCS) calibration and channel characterization. The single channel phase characterization showed that the system is coherent from pulse-to-pulse and hence can perform Doppler processing for pulse integration and clutter suppression. The phase difference between channels characterization showed that the system is coherent between channels, and hence can perform angle-of-arrival (AOA) processing for angular estimation.

Earlier work has shown that the system's detection ranges for large airliners as 5.5km and a small aircraft as 2.8km. Experiments have shown a detection range of a small unmanned aerial vehicle (UAV) as more than 350m. An experiment was conducted tracking a small UAV with a method of adaptive track update interval implemented. This illustrated that the system can autonomously adapt its processing in real-time. Parameters that can be adapted at runtime are; carrier frequency, bandwidth, pulse length, pulse repetition frequency (PRF) and number of pulses in dwell.

The field of cognitive and adaptive radar research is dependent on radar testbeds to perform experiments in real-time. In these systems, radar parameters selection is dependent on the scene the radar observes. In order to validate algorithms it is therefore necessary to perform real-world experiments. Such a testbed should be able to adapt its parameters on-the-fly, such as PRF, pulse length, bandwidth, waveform type, number of pulses in burst and carrier frequency, in order to adapt its performance based on the radar perception. This USRP based testbed presented here is a demonstration of how such a testbed can be produced on a low budget.

References

[1] K. L. Bell, C. J. Baker, G. E. Smith, J. T. Johnson, and M. Rangaswamy, "Cognitive Radar Framework for Target Detection and Tracking," *IEEE Journal of Selected Topics in Signal Processing*, vol. 4553, no. c, pp. 1–1, 2015.

[2] A. E. Mitchell, G. E. Smith, K. L. Bell, A. J. Duly, and M. Rangaswamy, "Fully adaptive radar for variable resolution imaging," in *International Conference on Radar Systems (Radar 2017)*, vol. 1, no. 1, Oct 2017, pp. 1–6.

Dette er en postprint-versjon/This is a postprint version.
DOI til publisert versjon/DOI to published version: 10.1109/MAES.2019.2953803

[3] G. E. Smith, Z. Cammenga, A. Mitchell, K. L. Bell, J. Johnson, M. Rangaswamy, and C. J. Baker, "Experiments with cognitive radar," *IEEE Aerospace and Electronic Systems Magazine*, vol. 31, no. 12, pp. 34–46, 2016.

[4] A. E. Mitchell, G. Smith, K. L. Bell, A. Duly, and M. Rangaswamy, "Hierarchical Fully Adaptive Radar," *IET Radar, Sonar & Navigation*, vol. 12, no. February, p. 12, 2018. [Online]. Available: http://digital-library.theiet.org/content/journals/10.1049/iet-rsn.2018.5339

[5] A. E. Mitchell, G. E. Smith, K. L. Bell, A. J. Duly, and M. Rangaswamy, "Cost function design for the fully adaptive radar framework," *IET Radar, Sonar Navigation*, vol. 12, no. 12, pp. 1380–1389, 2018.

[6] "Ettus USRP site," https://www.ettus.com/, Accessed: 27.03.2019.

[7] A. Prabaswara, A. Munir, and A. B. Suksmono, "GNU Radio based software-defined FMCW radar for weather surveillance application," in *Proceedings of 2011 6th International Conference on Telecommunication Systems, Services, and Applications, TSSA 2011*, 2011, pp. 227–230.

[8] H. O. Moreno, F. Spadafora, P. Pace, V. Loscri, G. Di Massa, A. Costanzo, G. Aloi, S. Costanzo, and A. Borgia, "Potentialities of Usrp-Based Software Defined Radar Systems," *Progress In Electromagnetics Research B*, vol. 53, no. December, pp. 417–435, 2014.

[9] B. Bleszynski, "A simple radar based on USRP software defined radio," *2017 Signal Processing Symposium, SPSympo 2017*, no. 1, pp. 1–4, 2017.

[10] B. H. Kirk, J. W. Owen, R. M. Narayanan, S. D. Blunt, A. F. Martone, and K. D. Sherbondy, "Cognitive software defined radar: waveform design for clutter and interference suppression," in *SPIE Defense + Security*, vol. 10188, no. May 2017, Anaheim, 2017.

[11] J. M. Christiansen, G. E. Smith, and K. E. Olsen, "USRP based cognitive radar testbed," in *2017 IEEE Radar Conference, RadarConf 2017*, 2017.

[12] J. M. Fuster, *Cortex And Mind Unifying Cognition*. Oxford University Press, 2003.

[13] "MiniCircuits ZVE-8G+ HPA Datasheet," https://www.minicircuits.com/pdfs/ZVE-8G+.pdf, Accessed: 29.06.2016.

[14] "MiniCircuits Modern Amplifier Terms Defined," https://www.minicircuits.com/pages/pdfs/amp3-4.pdf, Accessed: 23.08.2016.

[15] B. Dixon, R. Pollard, and S. Iexekiel, "A discussion of the effects of amplifier back-off on OFDM." Institute of Electrical and Electronics Engineers (IEEE), jan 2003, pp. 14–19.

[16] "Python UHD wrapper," https://kb.ettus.com/UHD_Python_API, Accessed: 15.03.2019.

[17] "USRP Hardware driver website," https://www.ettus.com/sdr-software/detail/usrp-hardware-driver, Accessed: 16.08.2016.

[18] "Qt website," http://www.qt.io, Accessed: 16.08.2016.

[19] "Qwt website," http://qwt.sourceforge.net, Accessed: 16.08.2016.

[20] "Boost C++ libraries website," http://www.boost.org, Accessed: 16.08.2016.

[21] "NVIDIA CUDA Website," http://www.nvidia.com/object/cuda_home_new.html, Accessed: 26.07.2017.

[22] H. Rohling, "Ordered Statistic CFAR Technique – an Overview," *Processing*, pp. 631–638, 2011.

[23] M. A. Richards, J. A. Scheer, and W. A. Holm, *Principles of Modern Radar, Volume I - Basic Principles*. SciTech Publishing, 2010.

[24] R. Schmidt and X. W. Af, "Multiple Emitter Location and Signal Parameter," *IEEE Transactions on Antennas and Propagation*, vol. 34, no. 3, pp. 276–280, 1986. [Online]. Available: http://ieeexplore.ieee.org/lpdocs/epic03/wrapper.htm?arnumber=1143830

[25] S. Bordonaro, P. Willett, and Y. Bar-Shalom, "Consistent Linear Tracker with Converted Range, Bearing, and Range Rate Measurements," *IEEE Transactions on Aerospace and Electronic Systems*, vol. 53, no. 6, pp. 3135–3149, 2017.

[26] J. M. Christiansen, K. E. Olsen, and G. E. Smith, "Fully adaptive radar for track update-interval control," in *2018 IEEE Radar Conference (RadarConf18)*, April 2018, pp. 0400–0404.

Dette er en postprint-versjon/This is a postprint version.
DOI til publisert versjon/DOI to published version: 10.1109/MAES.2019.2953803